



A Method for Characterizing the Degree of Inter-particle Bond Formation in Cold Sprayed Coatings

T.S. Price, P.H. Shipway, D.G. McCartney, E. Calla, and D. Zhang

(Submitted June 15, 2007; in revised form July 23, 2007)

The degree of bonding between particles within cold-sprayed deposits is of great importance as it affects their mechanical and physical properties. This article describes a method for characterizing the bonding between aluminum and copper particles following deposition by cold spraying. Aluminum and copper powders were blended in the ratio 1:1 by volume, deposited onto a copper substrate and subsequently heat treated at 400 °C for 15 min. An intermetallic layer formed along some regions of the aluminum-copper boundaries, believed to be where true metal to metal contact had occurred. In other regions, metal to metal contact was inhibited by the presence of oxide films. Image analysis was employed to measure the fraction of the aluminum-copper interface covered with intermetallic phases and to estimate intermetallic thicknesses. By increasing the primary gas pressure in the cold-spray process, an increase in the degree of inter-particle bond formation was observed.

Keywords bonding, CGDS, cold spraying, particle impact

1. Introduction

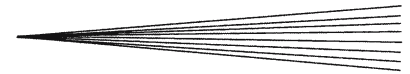
Cold gas dynamic spraying (CGDS) involves the acceleration and impact of solid particles with a substrate to form a coating; typically, deposit thicknesses range between 100 and 1500 μm . The particles are accelerated in a supersonic gas jet which can be produced by the use of a converging-diverging de Laval nozzle (Ref 1). Particles impinging on a substrate will either rebound from the substrate (with or without causing erosion) or bond with the substrate (Ref 2, 3), depending on the material type and particle velocity on impact with the substrate. It has been observed that for a range of metals, particle deposition occurs when the particle velocity exceeds a critical velocity (typically in excess of 500 m/s for materials such as aluminum, copper, and titanium) (Ref 2, 4).

The mechanism of coating build up is believed to involve initial impact-damage to the substrate which removes the oxide layer and allows impinging particles to bond with the newly exposed metal surface (Ref 5). A continued flux of impinging particles leads to further deposit build up through high velocity impacts between particles arriving at the substrate and those already deposited. The occurrence of bonding on particle impact is widely regarded to be related to the occurrence of shear

instabilities at the interparticle boundaries, due to high strain rate deformation.

Much effort has been devoted to improving our understanding of the mechanisms of coating build up through finite element modeling of particle impacts and microstructural analysis of the associated deformation (Ref 2, 4, 6). This has shown that on impact, high plastic strain rates can occur in the immediate vicinity of the contact zone which lead to adiabatic heating, localized softening of the material and the formation of what are termed shear instabilities. A consequence of this is that solid-state jets of metal are predicted to be extruded from the interface between an impinging particle and the material on the substrate. Such features have been clearly observed by a number of researchers (Ref 2, 4, 6-12). It is the formation of the solid-state jets which, it is argued, result in the removal of the surface oxide layer and allow true metal-to-metal contact, i.e., metallic bond formation. Formation of intermetallic compounds between a suitably reactive substrate and deposit materials has also been observed (Ref 13). Assadi et al. (Ref 4) briefly considered the interaction between multiple spherical particles impacting a surface and showed that previous particle impacts to a substrate do indeed affect the shear instabilities generated in further impinging particles. Additionally, the strain and temperature distribution at the particle-particle impact interface was shown to be inhomogeneous; they suggested that this would indicate that bonding may be confined to a fraction of the interacting surfaces. This could, potentially, be due to oxide layers not being sufficiently broken down on particle impact. While shear and temperature effects can readily be considered when modeling particle impacts, the role of surface oxides in modifying interface interactions has not been addressed in detail, even though its role is widely recognized (Ref 2).

T.S. Price, P.H. Shipway, D.G. McCartney, E. Calla, and D. Zhang, School of Mechanical, Materials and Manufacturing Engineering, University of Nottingham, Nottingham, UK. Contact e-mail: Philip.Shipway@nottingham.ac.uk.



Experimental work to characterize interparticle boundaries in cold-sprayed coatings presents a number of challenges and a range of techniques have been employed to determine, whether oxide free boundaries do indeed exist (Ref 5, 8, 10, 14-16). A number of authors have reported metallographic studies using scanning and transmission electron microscopy and have shown that, although particles appear well bonded, interparticle defects do exist in the form of voids, pores and sub-micron oxide layers. There has also been evidence presented for the presence of surface oxides ruptured during deposition. Etching of the coating microstructure, to highlight the defects surrounding individual particles, has been carried out on aluminum (Ref 5, 15) and copper (Ref 8) cold sprayed coatings. Stoltenhoff et al. (Ref 8) used this approach, combined with image analysis, to estimate the degree of metal-to-metal contact between splats for deposits sprayed with nitrogen and helium gases. For particles sprayed with helium gas (and therefore an expected higher impact velocity), 75% of interfaces were found to show metallic bonding compared to 30 to 35% for deposits sprayed with nitrogen gas. They also showed that the amount of deformation that occurred was non-uniform within the particle and was predominantly found close to surfaces that are impacted by further impinging particles. While this etching technique provides useful insight, control of the etching behavior to obtain reproducible results is very difficult.

The nature of the oxide layers between individual particles in aluminum, copper, and nickel deposits has also been analyzed using transmission electron microscopy (Ref 10, 14, 16). It was found that at inter-particle boundaries oxides were identified that appeared to have originated from the original feedstock. Although evidence of ruptured surface oxides was found, which allowed true metal-to-metal contact to occur at points along particle interfaces, true metal to metal bonding was incomplete (Ref 16).

Clearly, defects will affect the mechanical and physical properties of a cold-sprayed coating and thus it is important to be able to characterize inter-particle bond formation and assess how it is affected by deposition conditions. The present study was therefore designed to investigate the interparticle bonding between aluminum and copper particles following deposition by cold spraying. The approach adopted was to spray a blended powder comprising elemental Al and Cu particles and to subsequently anneal the deposit at 400 °C. Since intermetallic phases form rapidly by inter-diffusion at this temperature in the Al-Cu system when oxide free metal surfaces are in contact (Ref 17-19), then the extent of intermetallic phase formation can act as a marker for interfaces without oxide. Furthermore, image analysis was used to quantify the degree of interparticle bonding in deposits sprayed under different conditions.

2. Experimental Methods

2.1 Materials

Commercial purity (>99 wt.%) copper (Sandvik Osprey, Neath, UK) and aluminum (Aluminum Powder

Company Ltd, Sutton Coldfield, UK) powders were employed to produce the coatings. The copper had a nominal size range $-25+5\ \mu\text{m}$ and the size range of the aluminum was $-45+15\ \mu\text{m}$. In order to prepare the feedstock for spray deposition, these powders were mechanically blended in the ratio 1:1 by volume using a three-dimensional Turbula mixer (Glen Creston, Middlesex, UK) for 30 min. The blended powder was sprayed onto commercial purity copper substrates of dimensions $16\ \text{mm}\times 120\ \text{mm}\times 1.6\ \text{mm}$ which had a ground surface finish with an average surface roughness, Ra, of $0.9\ \mu\text{m}$.

2.2 Spray Deposition and Heat Treatment

CGDS utilized a de Laval nozzle with a 100 mm long diverging section, a throat diameter of $\sim 1.35\ \text{mm}$ and an area expansion ratio of ~ 8.8 . Room temperature helium was used as the primary accelerating gas and nitrogen as the powder carrier gas. The carrier gas pressure was normally set to approximately 1 bar above that of the primary gas. A high-pressure powder feeder (Praxair 1264HP, Indianapolis, IN, USA) was employed with a powder feed wheel containing 120 holes rotating at a speed of 4 rpm. This gave a powder feed rate of approximately 60 g/min when using pure copper powder. Prior to spraying, the copper substrate was degreased with alcohol and clamped to a table so that the distance between the CGDS nozzle exit and the substrate was fixed at 20 mm. The nozzle was positioned vertically above an X-Y traverse unit and was traversed relative to the substrate at $500\ \text{mm s}^{-1}$. A coating was deposited, centrally, onto an area measuring $80\ \text{mm}\times 16\ \text{mm}$ by making a series of overlapping passes. Typically, four traverses of the gun were required to build up a deposit $\sim 900\ \mu\text{m}$ thick. Coatings were thus prepared at two primary gas pressures of 15 and 29 bar using helium.

Following spray deposition, samples (coating plus substrate) were heat treated in a tube furnace (Lenton Furnaces, Sheffield, UK). The furnace was evacuated using a rotary pump prior to heating and heat treatment was performed under a continuous flow of high-purity argon gas. Samples were heated at $20\ \text{°C/min}$ to the annealing temperature of $400\ \text{°C}$, held at this temperature for 15 min and then furnace cooled to room temperature. The furnace cooled at a rate of approximately $10\ \text{°C/min}$ from the annealing temperature, $400\ \text{°C}$ to $350\ \text{°C}$. Samples sprayed with the two primary gas pressures were heat treated in the same run to allow direct comparison.

2.3 Microstructural Characterisation

For microstructural investigation, deposit samples were mounted in conducting resin, sequentially ground using SiC paper and polished first to a $1\ \mu\text{m}$ diamond surface finish and then with colloidal SiO_2 . A Philips/FEI XL30 and FEG-ESEM (FEI Europe, Eindhoven, The Netherlands) scanning electron microscope (SEM) operated at 20 kV was employed to examine the microstructures of the as-sprayed and heat-treated deposits using the back-scattered electron (BSE) signal to form the image. This provides contrast, which is dependent, primarily, on the

mean atomic number of the phases present. EDX analysis was carried out to characterize the intermetallics found between aluminum and copper splats.

For samples sprayed at 15 or 29 bar and subsequently heat treated, two characteristic features were examined to quantify the extent of intermetallic phase formation at the interfaces between copper and aluminum particles. First, the fraction of the total Al-Cu interface length where an intermetallic phase had formed was measured and secondly, the average intermetallic layer thickness was determined. These measurements were made using the analysis software ImageJ (U.S. National Institutes of Health, Bethesda, Maryland, USA). For each stagnation gas pressure, up to four BSE images at a magnification of 4000 \times , representative of the coating microstructure, were selected for quantitative analysis. All visible interface lengths and corresponding intermetallic lengths were measured. Lines were overlaid randomly across the microstructure, and the thickness of the intermetallic measured (perpendicular to the interface) at points where the lines intersected with any intermetallic region. Between 50 and 60 thickness measurements were made for each primary gas pressure.

3. Results and Discussion

Figure 1(a) and (b) show BSE images of the Al-Cu microstructure after being sprayed at 15 and 29 bar, respectively. The copper particles give brighter contrast in the image, due to their higher atomic number. In both figures there appears to be little porosity with good interparticle contact. There is no significant difference observable between the 15 and 29 bar deposits.

Following heat treatment of the deposits, it was found that one or more intermetallic phases form at interparticle boundaries but coverage of the Al-Cu interfaces is incomplete. This is shown in Fig. 2(a) and (b) for the 15 and 29 bar primary gas pressures, respectively. It can be seen that, although intermetallic layers are apparently absent from some interfacial regions, they had grown to a few microns in thickness in other areas. This is shown in more detail in Fig. 3. Three different intermetallic phases have been found between a copper and aluminum splat, shown as intermediate gray levels (Fig. 3). The intermetallic phases are numbered 1, 2 and 3, with phase 1 closest to the copper splat and phase 3 closest to the aluminum. Phases 1 and 3 were identified by EDX analysis as Cu_3Al_2 (δ – 60 at.% Cu) and CuAl_2 (θ – 33 at.% Cu) respectively. Phase 2 was harder to accurately characterize due to its thickness being close to the spatial resolution of EDX analysis. However, both the BSE image and EDX analysis qualitatively indicate that this phase has a composition between that of phases 1 and 3. A previous interdiffusion study showed that up to five possible intermetallic phases may be expected for an aluminum-copper system ranging from Cu_9Al_4 (γ_2) to CuAl_2 (θ) (Ref 18). Not all five intermetallic phases were identified within the current samples; however, it may be postulated that phase 2 is CuAl (η_2 – 50 at.% Cu) or Cu_4Al_3 (ζ_2 – 57.1 at.% Cu).

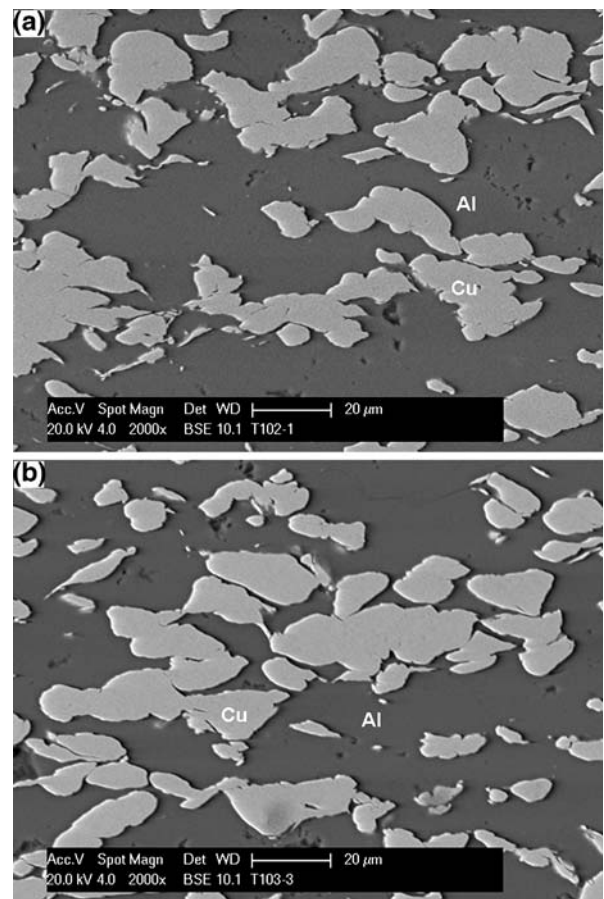


Fig. 1 BSE images of the as-sprayed Al-Cu deposits using a primary gas pressure of (a) 15 bar and (b) 29 bar showing Cu (bright), Al (dark) and no evidence for intermetallic phase at the interface. Spray direction top to bottom

Quantitative measurements with ImageJ showed a significant difference between the deposits produced at the two different gas pressures following heat treatment. At 15 bar primary gas pressure, the average intermetallic layer thickness was found to be $1.1 \pm 0.1 \mu\text{m}$ and the fraction of the interface length covered with intermetallic was 0.44 ± 0.05 . For the 29 bar primary gas pressure, the corresponding values for thickness and fractional coverage were $2.0 \pm 0.1 \mu\text{m}$ and 0.74 ± 0.05 , respectively; a significant increase compared with the deposits made at 15 bar. It was also found that the development of the intermetallic layer did not depend on interface orientation with respect to the impact direction.

The reason for incomplete coverage of Al-Cu interfaces with an intermetallic layer can be attributed to oxide layers on the surfaces of one or both original feedstock powders which act as a diffusion barrier. Aluminum, in particular, forms an oxide which is thermodynamically very stable and so bonding of Al and Cu particles is potentially difficult, even at elevated temperature, unless this oxide film can be broken and intimate metal to metal contact obtained. In this respect the occurrence of shear instabilities when high velocity particle impact occurs has

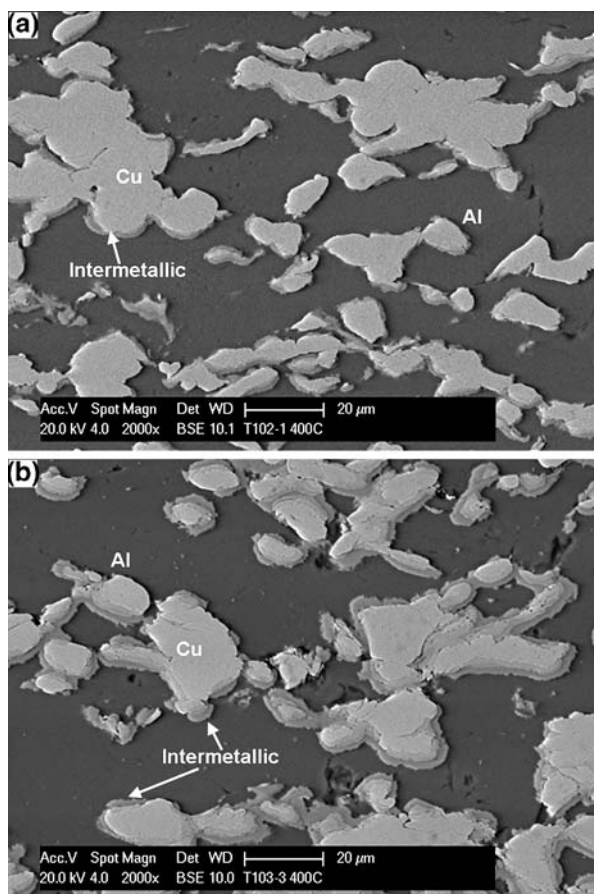


Fig. 2 BSE images of the heat-treated Al-Cu deposits which were sprayed at (a) 15 bar and (b) 29 bar showing Cu (bright), Al (dark) and an intermetallic layer of intermediate contrast at the interface. Spray direction top to bottom

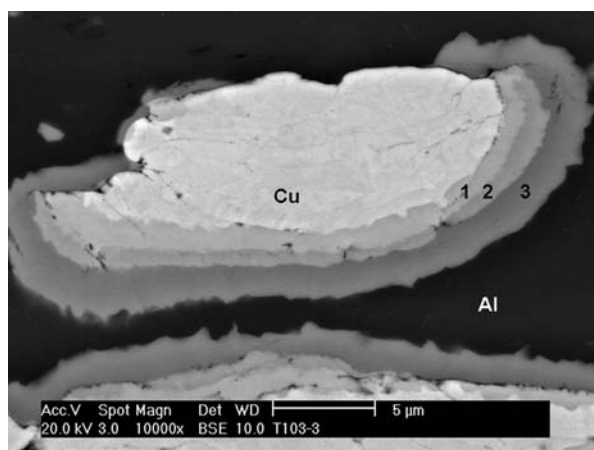


Fig. 3 BSE image of the heat treated Al-Cu deposit sprayed at 29 bar at high magnification showing Cu, bright, Al, dark, and three distinct intermetallic layers at the interface. Spray direction top to bottom

a key role in breaking down oxide films and creating intimate metallic contact which will favor atomic level bonding during elevated temperature annealing. The

increase in fractional interface coverage with increasing primary gas pressure, which was measured in this work can presumably be attributed to more extensive breakdown of oxide films at the higher pressure. This is because particle velocity increases with primary gas pressure which in turn creates more extensive regions of shear instability as predicted by finite element modeling (Ref 4). Thus it can be concluded that a higher particle velocity in the CGDS process causes a greater degree of direct metal contact between particles to be achieved in the deposit. The phenomenon of localized regions of intermetallic layer formation, related to oxide breakdown, has also been observed in the context of studies on diffusion bonding of Al and Cu (Ref 19). In this work, it was noted that an increase in bonding pressure increased the area over which intermetallics formed, because of increased oxide break-up.

The intermetallic layer development during elevated temperature annealing can be explained in terms of a solute diffusion controlled process. It was established by Manna et al. (Ref 17) and Funamizu et al. (Ref 18) that the growth kinetics follow the following equation:

$$w = \sqrt{k \cdot t} \quad (\text{Eq 1})$$

where w is the intermetallic thickness, t is the dwell time of the heat treatment in seconds and k is the rate constant. k is temperature dependent and is given by:

$$k = k_0 \cdot \exp\left(-\frac{Q}{R \cdot T}\right) \quad (\text{Eq 2})$$

where k_0 is the pre-exponential constant, Q is the activation energy of the process, R is the gas constant and T is the absolute temperature. Data for calculating k are given in Table 1 for molten aluminum deposited by hot dipping onto a copper substrate with and without prior cold work (Ref 17). Using the values given, the layer thicknesses estimated for the present annealing treatment are ~ 1 and $6 \mu\text{m}$ for the assumption of 0 and 40% cold work, respectively. These values are in reasonable agreement with those observed experimentally in this work.

The increased intermetallic layer thickness obtained with the higher primary gas pressure can also be explained on the basis of the work of Manna et al. (Ref 17) in which growth kinetics were found to increase with increasing cold work due to crystal defects increasing solute diffusivity. It is well known that particles in cold-sprayed deposits possess significant microstrain due to dislocations and other lattice defects (Ref 20). Since the degree of

Table 1 Data used to calculate the intermetallic layer growth between aluminum and copper for following heat treatment

| Condition of copper substrate | Pre-exponential factor (k_0)/ m^2/s | Activation energy (Q)/ kJ/mol |
|-------------------------------|---|--|
| No prior deformation | 0.9×10^{-4} | 136.9 |
| 40% prior deformation | 0.4×10^{-4} | 116.6 |
| Taken from reference (Ref 17) | | |

microstrain, i.e., defect density, is likely to increase with increased particle impact velocity if the primary gas pressure is increased, then this is expected to lead to an increase in intermetallic layer growth on annealing.

Finally, the methodology reported here could also be used to investigate the level of bonding between a substrate and coating if two dissimilar materials are employed and where an intermetallic layer is known to form during elevated temperature annealing. It is argued that initial particle impacts act to condition the substrate by removing a pre-existing oxide layers and particles which arrive subsequently are then able to form a bond. It could thus be expected that oxide is not removed completely from the substrate surface and, therefore, bonding between substrate and depositing particles is not uniform but contains weak links.

4. Conclusions

A method for characterizing the bonding between aluminum and copper powder particles following deposition by cold spraying has been developed. An intermetallic layer is observed to form at particle boundaries following a short annealing treatment at 400 °C but the coverage of particle interfaces is found to be nonuniform. This is attributed to the incomplete breakup of oxide films which act as diffusion barriers and provides a good indication of the degree of metal to metal contact in the as-sprayed deposit. By increasing particle velocity in the CGDS process a greater degree of direct metal contact between particles in the deposit is achieved.

Acknowledgments

T.S. Price acknowledges financial support from the Nottingham Innovative Manufacturing Research Centre (NIMRC) and the EPSRC in the form of a Ph.D. studentship.

References

1. R.C. Dykhuizen and M.F. Smith, Gas Dynamic Principles of Cold Spray, *J. Therm. Spray Technol.*, 1998, **7**, p 205-212
2. T. Schmidt, F. Gartner, H. Assadi, and H. Kreye, Development of a Generalized Parameter Window for Cold Spray Deposition, *Acta Mater.*, 2006, **54**, p 729-742
3. S.V. Klinkov, V.F. Kosarev, and M. Rein, Cold Spray Deposition: Significance of Particle Impact Phenomena, *Aerosp. Sci. Technol.*, 2005, **9**, p 582-591
4. H. Assadi, F. Gartner, T. Stoltenhoff, and H. Kreye, Bonding Mechanism in Cold Gas Spraying, *Acta Mater.*, 2003, **51**, p 4379-4394
5. T.H. Van Steenkiste, J.R. Smith, and R.E. Teets, Aluminum Coatings Via Kinetic Spray with Relatively Large Powder Particles, *Surf. Coat. Technol.*, 2002, **154**, p 237-252
6. M. Grujicic, C.L. Zhao, W.S. DeRosset, and D. Helfritsch, Adiabatic Shear Instability Based Mechanism for Particles/Substrate Bonding in the Cold-Gas Dynamic-Spray Process, *Mater. Design*, 2004, **25**, p 681-688
7. R.C. Dykhuizen, M.F. Smith, D.L. Gilmore, R.A. Neiser, X. Jiang, and S. Sampath, Impact of High Velocity Cold Spray Particles, *J. Therm. Spray Technol.*, 1999, **8**, p 559-564
8. T. Stoltenhoff, C. Borchers, F. Gartner, and H. Kreye, Microstructures and Key Properties of Cold-Sprayed and Thermally Sprayed Copper Coatings, *Surf. Coat. Technol.*, 2006, **200**, p 4947-4960
9. V.K. Champagne, D. Helfritsch, P. Leyman, S.G. Ahl, and B. Klotz, Interface Material Mixing Formed by the Deposition of Copper on Aluminum by Means of the Cold Spray Process, *J. Therm. Spray Technol.*, 2005, **14**, p 330-334
10. C. Borchers, F. Gartner, T. Stoltenhoff, and H. Kreye, Microstructural Bonding Features of Cold Sprayed Face Centered Cubic Metals, *J. Appl. Phys.*, 2004, **96**, p 4288-4292
11. J.W. Wu, H.Y. Fang, S. Yoon, H. Kim, and C. Lee, The Rebound Phenomenon in Kinetic Spraying Deposition, *Scripta Mater.*, 2006, **54**, p 665-669
12. T. Stoltenhoff, H. Kreye, and H.J. Richter, An Analysis of the Cold Spray Process and its Coatings, *J. Therm. Spray Technol.*, 2002, **11**, p 542-550
13. A. Bolesta, V.M. Fomin, M.R. Sharafutdinov, and B.P. Tolochko, Investigation of Interface Boundary Occurring During Cold Gas-Dynamic Spraying of Metallic Particles, *Nucl. Instrum. Meth. Phys. Res. Sec. A-Accelerat. Spectrom. Detect. Assoc. Equip.*, 2001, **470**, p 249-252
14. R.C. McCune, W.T. Donlon, O.O. Popoola, and E.L. Cartwright, Characterization of Copper Layers Produced by Cold Gas-Dynamic Spraying, *J. Therm. Spray Technol.*, 2000, **9**, p 73-82
15. R. Morgan, P. Fox, J. Pattison, C. Sutcliffe, and W. O'Neill, Analysis of Cold Gas Dynamically Sprayed Aluminium Deposits, *Mater. Lett.*, 2004, **58**, p 1317-1320
16. K. Balani, A. Agarwal, S. Seal, and J. Karthikeyan, Transmission Electron Microscopy of Cold Sprayed 1100 Aluminum Coating, *Scripta Mater.*, 2005, **53**, p 845-850
17. I. Manna and J.D. Majumdar, Enhanced Kinetics of Diffusion Coating of Aluminum on Copper by Boundary Diffusion, *J. Mater. Sci. Lett.*, 1993, **12**, p 920-922
18. Y. Funamizu and K. Watanabe, Interdiffusion in Al-Cu System, *Trans. Jpn. Inst. Metals*, 1971, **12**, p 147-152
19. F.A. Calvo, A. Urena, J.M.G. Desalazar, and F. Molleda, Special Features of the Formation of the Diffusion Bonded Joints between Copper and Aluminum, *J. Mater. Sci.*, 1988, **23**, p 2273-2280
20. E. Calla, D.G. McCartney, and P.H. Shipway, Effect of heat treatment on the structure and properties of cold sprayed copper. In *Thermal Spray 2005: Advances in Technology and Application*. DVS, Basel, Switzerland, 2005